Письма в ЭЧАЯ. 2014. Т. 11, № 4(188). С. 784–795

DETERMINATION OF IVC BREAKPOINT FOR JOSEPHSON JUNCTION STACK. NON-PERIODIC BOUNDARY CONDITIONS WITH $\gamma = 1$

S. I. Serdyukova [1]

Joint Institute for Nuclear Research, Dubna

We prove that, in the case of non-periodic (with $\gamma = 1$) boundary conditions, the calculation of the current-voltage characteristic (IVC) for a stack of n intrinsic Josephson junctions reduces to solving a system of $[(n+1)/2]$ nonlinear differential equations instead of the n original ones. The current-voltage characteristic $V(I)$ has the shape of a hysteresis loop. On the back branch of the loop, $V(I)$ decreases to zero rapidly near the breakpoint I_b. We managed to derive an algorithm determining the approximate breakpoint location and to improve simultaneously the mixed numerical-analytical algorithm of IVC calculation for a stack of Josephson junctions developed by us before. The efficiency of the improved algorithm is shown by the calculations of IVC for stacks consisting of various numbers of intrinsic Josephson junctions.

Доказано, что в случае непериодических (с $\gamma = 1$) граничных условий вычисление вольт-амперной характеристики (ВАХ) для системы n внутренних джозефсоновских переходов сводится к решению $[(n+1)/2]$ нелинейных дифференциальных уравнений вместо n оригинальных. Вольт-амперная характеристика $V(I)$ имеет вид петли гистерезиса. На обратной ветви петли гистерезиса значение $V(I)$ быстро спадает к нулю в окрестности точки излома I_b. Нам удалось разработать алгоритм, определяющий приближенное значение точки излома $\tilde{I}_b$, и одновременно улучшить развитый нами ранее смешанный численно-аналитический алгоритм вычисления ВАХ для систем джозефсоновских переходов. Эффективность улучшенного алгоритма продемонстрирована на примере вычисления ВАХ для систем с различным числом внутренних джозефсоновских переходов.

PACS: 60.64

INTRODUCTION

A detailed investigation of the breakpoint current I_b and the breakpoint region width gives important information concerning the occurrence of longitudional plasma waves and the peculiarities of stacks with a finite number of intrinsic Josephson junctions [1–3]. The breakpoint region in the current-voltage characteristics (IVC) follows from the solution of the system of n dynamical equations of the phase differences for a stack of n intrinsic Josephson junctions. In this work we prove that, in the case of non-periodic (with $\gamma = 1$) boundary conditions, the IVC calculation for a stack of n intrinsic Josephson junctions reduces to solving

[1] E-mail: sis@jinr.ru

a system of $[(n+1)/2]$ nonlinear differential equations instead of the n original ones. Solving this system on the interval $[0, T_{\max}]$ for different I, we get the current-voltage characteristic $V(I)$ as a hysteresis loop. First the Cauchy problem with the zero initial conditions is solved. For each next $I = I_{k+1}$, the already found $\psi(I_k, T_{\max})$ and $\dot{\psi}(I_k, T_{\max})$ are used as initial data. On the back branch of the hysteresis loop, voltage $V(I)$ decreases to zero rapidly near the breakpoint I_b [3]. Effective numerical and analytical methods for IVC calculation were developed in [4]. In [5] an equation determining the approximate breakpoint location in the case of periodic and non-periodic (with $\gamma = 0$) boundary conditions was developed. Now we report an algorithm which finds the approximate breakpoint location in the more complicated case of non-periodic (with $\gamma = 1$) boundary conditions and improves, at the same time, the mixed numerical-analytical method proposed in [4]. The improved mixed method showed excellent results in IVC calculation for stacks with different number of intrinsic Josephson junctions. Moreover, the calculation time reduced by an order of magnitude. The calculations were performed by using the REDUCE 3.8 system. As a matter of fact, this paper is a second part of [5], where the mathematical formulation of the hysteresis calculation problem and the system transformation was given in general form in Secs. 1 and 2, respectively. Omitting the details reported in [5], we directly start this work from spectral data of matrix A in the considered case of non-periodic boundary conditions with $\gamma = 1$. In Sec. 2 we prove three lemmas. Lemmas 1 and 3 enable the reduction of the problem to the solution of $[(n+1)/2]$ nonlinear differential equations instead of n original ones. Lemma 2 is a fundamental point for the long-time «asymptotic» construction, reported in Sec. 3. In Sec. 4 we present an improved analytical method of voltage V calculation which made it possible to define the approximate breakpoint location in the considered case of non-periodic boundary conditions with $\gamma = 1$. In Sec. 5 we discuss the results of the Josephson loop calculations for different n.

1. THE SPECTRAL DATA. THE SYSTEM TRANSFORMATION

The solution of the system

$$\ddot{\phi}_l = \sum_{l'=1}^{n} A_{l,l'}(I - \sin(\phi_{l'}) - \beta\dot{\phi}_{l'}), \qquad l = 1, \ldots, n, \tag{1}$$

for different I: $I = I_0 + k\Delta I \leqslant I_{\max}$; $I = I_{\max} - k\Delta I$, yields the current-voltage characteristics of stacks as hysteresis loops [3]. For the initial value of the current, $I = I_0$, the system (1) is solved with zero initial data on an interval $[0, T_{\max}]$. For each next I: $I = I_{k+1}$, the found $\phi_l(I_k, T_{\max}), \dot{\phi}_l(I_k, T_{\max})$ are used as initial data.

In the case of non-periodic, with $\gamma = 1$, boundary conditions, the A matrix is three-diagonal,

$$A = \begin{pmatrix} 1+2\alpha & -\alpha & 0 & \ldots & 0 & 0 \\ -\alpha & 1+2\alpha & -\alpha & 0 & \ldots & 0 \\ 0 & -\alpha & 1+2\alpha & -\alpha & 0 & \ldots \\ \ldots & \ldots & \ldots & \ldots & \ldots & \ldots \\ 0 & \ldots & 0 & -\alpha & 1+2\alpha & -\alpha \\ 0 & 0 & \ldots & 0 & -\alpha & 1+2\alpha \end{pmatrix}. \tag{2}$$

Matrices of such kind have been previously noticed as well [6]. The eigenvalues and eigenvectors of A can be written down explicitly:

$$\lambda_j = 1 + 2\alpha(1 - \cos(j\theta)), \quad \theta = \frac{\pi}{n+1}, \qquad j = 1, \ldots, n;$$

$$E_j = \sqrt{\frac{2}{n+1}} \begin{bmatrix} \sin(j\theta) \\ \sin(2j\theta) \\ \vdots \\ \sin(nj\theta) \end{bmatrix}, \qquad j = 1, \ldots, n. \tag{3}$$

The fundamental matrices D, the columns of which are E_l, reduce the A-matrices to diagonal forms [8],

$$D^* A D = \Lambda = \operatorname{diag}(\lambda_1, \lambda_2, \ldots, \lambda_n).$$

After the change of variables

$$\phi_l = \sum_{l'=1}^{n} d_{l,l'} \psi_{l'}, \qquad V_l = \sum_{l'=1}^{n} d_{l,l'} W_{l'},$$

we get a system

$$\ddot{\psi}_l = -\lambda_l \beta \dot{\psi}_l + \lambda_l I S_l - \lambda_l \sum_{l'=1}^{n} d_{l',l} \sin(\phi_{l'}), \qquad l = 1, \ldots, n,$$

where S_l is the sum of the E_l elements,

$$S_l = \sum_{l'=1}^{n} d_{l',l}.$$

The equations determining voltages (see (4) and (5) in [3]) result in

$$\frac{\partial \psi_l}{\partial t} = \lambda_l W_l, \qquad \bar{W}_l = \frac{\psi_l(T_{\max}) - \psi_l(T_{\min})}{\lambda_l (T_{\max} - T_{\min})},$$

respectively, while the total voltage of the stack is given by

$$V = \sum_{l=1}^{n} S_l \bar{W}_l = \sum_{l=1}^{n} S_l \frac{\psi_l(T_{\max}) - \psi_l(T_{\min})}{\lambda_l (T_{\max} - T_{\min})}. \tag{4}$$

2. THREE LEMMAS

Let us remind that S_j is sum of elements of orthonormal eigenvector E_j of the matrix (2). The following lemma holds.

Lemma 1. *For odd j*

$$S_j = \sqrt{\frac{2}{n+1}} \cot \frac{\pi j}{2(n+1)} = \sqrt{\frac{2}{n+1}} \frac{\sin(j\theta)}{(1 - \cos(j\theta))}, \quad j = 1, 3, \ldots, 2k-1 \leqslant n. \tag{5}$$

And for even j, $j = 2, 4, \ldots, 2k \leqslant n$, $S_j = 0$.

Proof. Further on we denote $cn = \sqrt{2/(n+1)}$, ns is integer part of $(n+1)/2$, $ns = [(n+1)/2]$. Remark that $ns = n/2$ for even n and $ns = (n+1)/2$ for odd n. Using (5) and the well-known formula (3.6.2) of [9],

$$\sum_{k=1}^{n} \sin(k\theta) = \frac{\cos(\theta/2) - \cos((n+1/2)\theta)}{2\sin(\theta/2)},$$

after substituting in the last $j\theta$ instead of θ, we get

$$S_j = cn \sum_{k=1}^{n} \sin(kj\theta) = cn \frac{\cos(j\theta/2) - \cos((n+1/2)j\theta)}{2\sin(j\theta/2)} =$$
$$= cn \frac{\cos(j\theta/2) - \cos(\pi j - j\theta/2)}{2\sin(j\theta/2)} = cn \frac{\cos(j\theta/2) - (-1)^j \cos(j\theta/2)}{2\sin(j\theta/2)}.$$

Thus, $S_j = 0$ for even j, $j = 2, 4, \ldots, 2ns$. And $S_j = cn\cot(j\theta/2)$ for odd j, $j = 1, 3, \ldots, 2ns - 1$. The lemma is proved.

In the derivation of long-time asymptotic, the system of nonlinear differential equations is replaced by an equivalent system of integral equations, which is solved using simple iterations. We succeeded in obtaining suitable asymptotic formulas based on the following result.

Lemma 2. *For all $m = 1, 2, \ldots, n$ and for any n, the sums*

$$\Sigma_m = \sum_{j=1}^{n} d_{m,j} S_j$$

have the same value and, hence, coincide with $\Sigma_1 = 1$.

Proof. The lemma was proved in general case by induction on m with the use of simple trigonometric relations, specifically, for odd n

$$s_{m,n} = \sum_{k=1}^{ns} \cos(m(2k-1)\theta) = 0 \tag{6}$$

and for even n

$$s_{m,n} = \frac{(-1)^{m+1}}{2}. \tag{7}$$

For any m and n holds

$$s_{m,n} = \Re \frac{\exp[im\theta] - \exp[im(2ns+1)\theta]}{1 - \exp[2im\theta]}.$$

When n is odd, $2ns = n + 1$ and for any m

$$s_{m,n} = \Re \frac{1 + (-1)^{m+1}}{-2i\sin[m\theta]} = 0.$$

When n is even, $2ns = n$ and for any m

$$s_{m,n} = \Re \frac{1 + (-1)^{m+1} \exp[-im\theta]}{-2i \sin[m\theta]} = \frac{(-1)^{m+1}}{2}.$$

The relations (6) and (7) are proved. They imply that $s_{m,n} + s_{m+1,n} = 0$ for any m and n.

Additionally, we used the relation

$$\sum_{k=1}^{ns} \frac{\sin^2((2k-1)\theta)}{1 - \cos((2k-1)\theta)} = \frac{n+1}{2},$$

which holds for any m and n. Indeed,

$$\sum_{k=1}^{ns} \frac{\sin^2((2k-1)\theta)}{1 - \cos((2k-1)\theta)} = \sum_{k=1}^{ns} \frac{1 - \cos^2((2k-1)\theta)}{1 - \cos((2k-1)\theta)} = ns + s_{1,n}.$$

For odd n we have $ns = (n+1)/2$ and $s_{1,n} = 0$, hence $ns + s_{1,n} = (n+1)/2$.

And for even n we have $ns = n/2$ and $s_{1,n} = 1/2$, hence $ns + s_{1,n} = (n+1)/2$ again.

Suppose that the lemma holds for any m. Performing elementary trigonometric transformations, we get

$$\Sigma_{m+1} = \sum_{l=1}^{n} d_{m+1,l} S_l = \frac{2}{n+1} \sum_{k=1}^{ns} \frac{\sin((m+1)(2k-1)\theta) \sin((2k-1)\theta)}{1 - \cos((2k-1)\theta)} =$$
$$= \frac{2}{n+1} \sum_{k=1}^{ns} \left(\frac{\sin(m(2k-1)\theta) \cos((2k-1)\theta) \sin((2k-1)\theta)}{1 - \cos((2k-1)\theta)} + \right.$$
$$\left. + \frac{\cos(m(2k-1)\theta) \sin^2((2k-1)\theta)}{1 - \cos((2k-1)\theta)} \right).$$

Using $\cos(x)/(1 - \cos(x)) = -1 + 1/(1 - \cos(x))$ and $\sin^2(x)/(1 - \cos(x)) = 1 + \cos(x)$, we get

$$\Sigma_{m+1} = \Sigma_m + \frac{2}{n+1} \sum_{k=1}^{ns} (\cos(m(2k-1)\theta) + \cos((m+1)(2k-1)\theta)) =$$
$$= \Sigma_m + \frac{2}{n+1}(s_{m,n} + s_{m+1,n}) = \Sigma_m.$$

The lemma is proved.

Taking into account the trivial symmetry properties of E_l and the relations $S_l = 0$ for even l, it is easy to conclude that the solution of the system (1) with zero initial data is reduced to solving the following system of ns equations:

$$\frac{\partial^2 \psi_{2l-1}}{\partial t^2} = \lambda_{2l-1} \left(-\beta \frac{\partial \psi_{2l-1}}{\partial t} + S_{2l-1} I - \sum_{m=1}^{n} d_{m,2l-1} \sin(\phi_m) \right),$$
$$\phi_m = \sum_{k=1}^{ns} d_{m,2k-1} \psi_{2k-1}, \qquad l = 1, 2, \ldots, ns. \tag{8}$$

The other equations associated with $S_l = 0$ have the trivial solutions $\psi_{2l} = 0$; therefore, the number of equations was halved. As the proof we present the following result.

Lemma 3. *For all n, l, m and any ψ_j it holds that $\phi_m = \phi_{n+1-m}$, which implies the relations*

$$\sum_{m=1}^{n} d_{m,2l} \sin\left(\sum_{k=1}^{ns} d_{m,2k-1}\psi_{2k-1}\right) = 0.$$

The validity of this lemma follows from the trivial symmetry properties of E_l components:

$$d_{m,l} = \sqrt{\frac{2}{(n+1)}} \sin\left(\frac{\pi m l}{(n+1)}\right), \quad \sin\left(\frac{\pi(n+1-m)l}{(n+1)}\right) = (-1)^{l+1} \sin\left(\frac{\pi m l}{(n+1)}\right).$$

The sense of Lemma 3 was to show that the nonzero components ψ_{2j-1} with odd numbers give no contribution to the components with even numbers.

3. NUMERICAL-ANALYTICAL METHOD FOR CALCULATING IVC

The general scheme of the suggested numerical-analytical method of the hysteresis loop calculation is the following: the right branch of the hysteresis loop and the back branch (not nearing some finite distance to I_b) are calculated using the «asymptotic» formulas. The rest points $(I, V(I))$ of the hysteresis loop are calculated numerically using the fourth-order Runge–Kutta method [7].

The numerical-analytical method was used to calculate the IVC for a stack of 19 homogeneous Josephson junctions [4]. The hysteresis loop was calculated both numerically and with the use of the «asymptotic» formulas. For each value of I, the system (8) of ten nonlinear differential equations was first solved with zero initial data on the interval $[0, T_{\max}]$ by applying the fourth-order Runge–Kutta method. For each subsequent I, the found

$$\psi_{2l-1}(T_{t\max}), \frac{\partial\psi_{2l-1}}{\partial t}(T_{t\max}), \quad l = 1, \ldots, 10,$$

were used as initial data. Similar computations were performed using «asymptotic» formulas, which were calculated during the run. The voltages were calculated by formula (4).

The system (8) with initial data

$$\psi_{2l-1}(0) = d_1(2l-1), \qquad \frac{\partial\psi_{2l-1}}{\partial t}(0) = d_2(2l-1)$$

is equivalent to the system of ns integral equations ($ns = 10$)

$$\psi_{2l-1} = w_{2l-1}t + d_1(2l-1) + \frac{d_2(2l-1) - w_{2l-1}}{\beta\lambda_{2l-1}}\left(1 - \exp\left(-\beta\lambda_{2l-1}t\right)\right) -$$
$$- \frac{1}{\beta}\int_0^t \left(1 - \exp\left(-\beta\lambda_{2l-1}(t-s)\right)\right) \sum_{m=1}^{n} d_{m,2l-1} \sin\left(\sum_{k=1}^{ns} d_{m,2k-1}\psi_{2k-1}\right) ds, \quad (9)$$

where

$$l = 1, 2, \ldots, ns \quad \text{and} \quad w_{2l-1} = S_{2l-1} I/\beta.$$

For each I and given initial data the system (9) was solved using simple iterations starting with zero. The result obtained after three iterations was regarded [10] as «asymptotic» of the solution of the system (8) for large t. After the first iteration step, we obtained

$$\psi^1_{2l-1} = w_{2l-1} t + d_1(2l-1) + \frac{d_2(2l-1) - w_{2l-1}}{\beta \lambda_{2l-1}} = w_{2l-1} t + A^1_{2l-1}. \tag{10}$$

Every time we rejected the exponentially small (for large t) terms.

Since $w_{2l-1} = S_{2l-1} I/\beta$, Lemma 2 implies that $\sum\limits_{l=1}^{ns} d_{m,2l-1} w_{2l-1} = I/\beta$ for all m. In other words, $\phi^1_m = (I/\beta)t + B_m$. For brevity we use the notations $w = I/\beta$, $\psi^1_m = wt + B_m$. Evaluating integrals

$$\int_0^t (1 - \exp(-\beta(t-s))) \sin(\omega s + a) ds = \\ = \frac{\cos(a)}{\omega} - \frac{\beta \sin(\omega t + a)}{\beta^2 + \omega^2} - \frac{\beta^2 \cos(\omega t + a)}{\omega(\beta^2 + \omega^2)} + O(\mathrm{e}^{-\beta t}) \tag{11}$$

and after some algebra, we get

$$\psi^2_{2l-1} = w_{2l-1} t + A^2_{2l-1} + C_{2l-1} \sin(wt + D_{2l-1}), \qquad l = 1, \ldots, ns. \tag{12}$$

The functions $\sin(wt + a + c\sin(wt + d))$ were replaced by $\sin(wt + a)(1 - si^2/2) + \cos(wt + a) si (1 - si^2/6)$, where $si = c \sin(wt + d)$. It remained to transform the resulting trigonometric polynomials into linear combinations of functions of the form $\sin(kwt + d)$ and to calculate the integrals termwise. These «asymptotic» formulas were used in [4].

4. IMPROVED NUMERICAL-ANALYTICAL METHOD FOR CALCULATING IVC. APPROXIMATE BREAKPOINT LOCATION

The attempts to find an approximate breakpoint location by analogy with [5] were useless. The following remark helped to overcome the difficulty. Namely, it is sufficient to calculate $V(I)$ for different I, $I = 0.5$–$0.05j$, solving «analytically» the system (8) with zero initial data, until I_c, satisfying $V(I_c)V(I_c + 0.05) < 0$, is obtained. The obtained I_c is taken for the approximate breakpoint location. The results obtained in this way are in good agreement with the numerical ones. The key to the solution came from the definition of an alternative way to simplify the calculation of the voltage V. Apart from an accurate definition of the breakpoint location, the calculating time of the hysteresis loop for a stack of 19 Josephson junctions decreased more than 9 times (against 5 obtained in [4]), as compared to the program used in numerical calculations). Below we present the result of calculating $\tilde{I}_b = 0.3$ for the stack of 19 Josephson junctions.

```
vb :=
{{0.5,33.7167375273},{0.45,40.235725455},{0.4,63.5053115073},
{0.35,62.9218862448}, {0.3, - 0.0454510614144}}$
   shut "D:\brt\vbbx3.txt"$
```

The derivation of the improved algorithm of calculating $V(I)$ started from recalculating $\psi_{2l-1}(t)$. First we have

$$\psi^2_{2l-1} = \psi^1_{2l-1} + F_{2l-1}(t), \qquad l = 1, 2, \ldots, ns,$$

where

$$F_{2l-1}(t) = \sum_{\xi=1}^{n\xi} \left[B_{2l-1}(\xi) + C^1_{2l-1}(\xi) \sin\left(wt + D^1_{2l-1}(\xi)\right) + C^2_{2l-1}(\xi) \cos\left(wt + D^2_{2l-1}(\xi)\right) \right], \quad l = 1, \ldots, ns.$$

Instead of arriving at the compact formulas (12), we have simply rewritten (11) as

$$\int_0^t (1 - \exp(-\beta(t-s))) \sin(\omega s + a) ds = \frac{\cos(a)}{\omega} - \\ - \frac{\beta(\beta\cos(a) + \omega\sin(a))}{\omega(\omega^2+\beta^2)} \cos(\omega t) - \frac{\beta(\omega\cos(a) - \beta\sin(a))}{\omega(\omega^2+\beta^2)} \sin(\omega t) + O(\mathrm{e}^{-\beta t})$$

and instead of (12) we get at once

$$\psi^2_{2l-1} = \psi^1_{2l-1} + F_{2l-1}(t) = \psi^1_{2l-1} + A^2_{2l-1} + cs(2l-1)\cos(wt) + cc(2l-1)\sin(wt) = \\ = \psi^1_{2l-1} + A^2_{2l-1} + C_{2l-1}\sin(wt + D_{2l-1}), \quad l = 1, \ldots, ns. \quad (13)$$

Remark that $C_{2l-1} = \sqrt{cs(2l-1)^2 + cc(2l-1)^2}$ and $D_{2l-1} = \arctan(cs(2l-1)/cc(2l-1))$.

We denote $at(j) = \sum\limits_{l=1}^{ns} d_{j,2l-1} A^1_{2l-1}$, where A^1_{2l-1} are the free terms of ψ^1_{2l-1} (see (10)), and

$$ft(j) = \sum_{l=1}^{ns} d_{j,2l-1} F_{2l-1}, \quad j = 1, \ldots, n.$$

And let $pp(2l-1)$ be free terms of the trigonometric polynomials

$$\sum_{j=1}^{n} d_{j,2l-1} \left[\cos(wt + at(j)) \left(ft(j) - \frac{ft(j)^3}{6} \right) - \sin(wt + at(j)) \frac{ft(j)^2}{2} \right], \qquad l = 1, \ldots, ns.$$

After integrating we find

$$\psi^3_{2l-1} = \psi^2_{2l-1} - \frac{pp(2l-1)}{b} \left(t - \frac{\exp(-\beta\lambda_{2l-1} T_{\min})}{\beta^2 \lambda_{2l-1}} \right), \qquad l = 1, \ldots, ns. \quad (14)$$

Taking into account (10) and (13), we obtain from (14) the «asymptotic» formulas of interest

$$\psi^3_{2l-1} = (w_{2l-1} + \delta_{2l-1})t + A^3_{2l-1} + C_{2l-1}\sin(wt + D_{2l-1}), \; l = 1, \ldots, ns. \quad (15)$$

The «analytical» method of IVC calculation means successive calculation of (10), (13), and (14) by the algorithm described above for every I_k and given initial data. As a result, the coefficients of (15) are determined.

Following (4), we obtain

$$V(I) = \sum_{l=1}^{ns} S_{2l-1} \frac{\psi^3_{2l-1}(T_{\max}) - \psi^3_{2l-1}(T_{\min})}{\lambda_{2l-1}(T_{\max} - T_{\min})}.$$

The calculations were performed for $\alpha = 0.2$, $\beta = 0.2$ by using the REDUCE 3.8 system [11] with $T_{\min} = 50$, $T_{\max} = 1000$, and a step $h = 0.1$ was chosen in the numerical calculations by means of the fourth-order Runge–Kutta method.

5. RESULTS OF THE CALCULATIONS

Figure 1 depicts the back branch of the hysteresis loop for $n = 19$. The solid and dotted lines, which are hardly distinguishable from each other at large I, refer to numerical and «analytical» calculations of the hysteresis loop, respectively. The numerical method of IVC calculation means that all points $(I_k, V(I_K))$ of the hysteresis loop (the whole right branch and the whole back branch) are calculated numerically using the fourth-order Runge–Kutta method. The «analytical» method of IVC calculation means that all points $(I_k, V(I_K))$ of the hysteresis loop (the right and the back branch) are calculated «analytically» using the «asymptotic» formulas.

In Fig. 2 the solid line is the same as in Fig. 1, while the circles on this line refer to the calculation performed by the following mixed numerical-analytical method. The whole right branch of the hysteresis loop, together with the back branch at $1.45 > I > 0.45 = 1.5\tilde{I}_b$, has been computed using the «asymptotic» formulas (15). The remaining points of the back

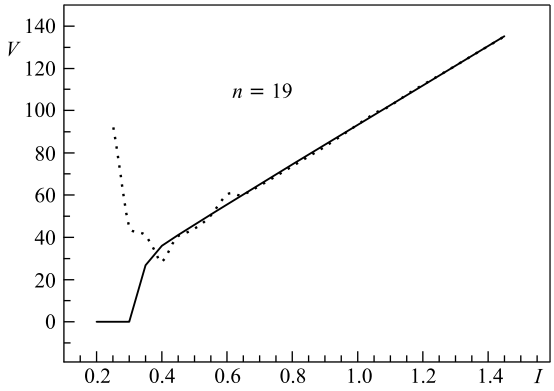

Fig. 1. The solid line refers to the back branch of the hysteresis loop for $n = 19$, calculated numerically: all points of the hysteresis loop have been calculated using the fourth-order Runge–Kutta method. The dotted line refers to the back branch of the hysteresis loop, calculated «analytically»: all points of the hysteresis loop have been calculated using the «asymptotic» formulas (15)

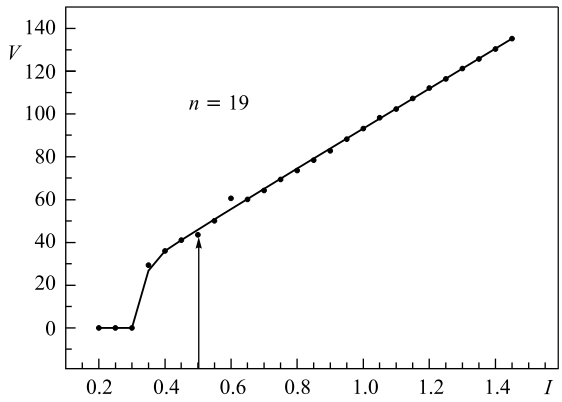

Fig. 2. The solid line refers to the back branch of the hysteresis loop calculated numerically for $n = 19$. The circles on this line refer to calculation performed by the mixed analytical-numerical method: the whole right branch of the hysteresis loop, together with the back branch at $1.45 > I > 0.45 = 1.5\tilde{I}_b$, has been computed using the «asymptotic» formulas (15). The points at $0.45 \geqslant I \geqslant 0.2$ were computed numerically by using the fourth-order Runge–Kutta method. The point $(0.5, 43.561\ldots)$, marked by the arrow, is the last point of the hysteresis loop calculated «analytically»

branch of the hysteresis loop were computed numerically by means of the fourth-order Runge–Kutta method. The point $(0.5, 43.561\ldots)$, marked in Fig. 2 by the arrow, is the last point of the hysteresis loop calculated «analytically». In spite of its seeming difference from the point $(0.5, 45.998)$ calculated numerically, the use of the «analytical» value as an input on the interval $[0.45, 0.2]$ of Fig. 2 results in points staying very close to the numerical curve. As a consequence, the numerical results of IVC calculation and the results obtained by the improved mixed numerical-analytical method are in good agreement with each other. It is worth noting that the shift from the pure Runge–Kutta method to the mixed method decreased the CPU time almost by an order of magnitude. For instance, the calculation of a single additional point using the Runge–Kutta method asks for 339640 ms CPU time, while the «analytical» computation of all points of the hysteresis loop takes 75759 ms only. The same calculations were performed for $n = 5, 9, 13, 19$, and $n = 25$. The corresponding outputs look similar to those in Figs. 1 and 2.

Surprisingly, the same $\tilde{I}_b = 0.3$ was obtained both at $n = 9$ and at $n = 19$. To clarify the problem, we have performed the similarity transform $(I_k, V(I_k, 9)V(1.45, 19)/V(1.45, 9))$ in Fig. 1 and this confidently reproduced the corresponding solid line. Here and below, $(I_k, V(I_k, n))$ are points of the back branch of the hysteresis loop for the stack of n intrinsic Josephson junctions, calculated numerically.

Further we made the hypothesis that all the considered $V(I_k, n)$ can be obtained from $V(I_k, 5)$. Figure 3 confirms this hypothesis. The solid lines in Fig. 3 refer to the back branches of the hysteresis loops calculated numerically for $n = 5, 9, 13, 19$, and $n = 25$, from bottom to top, respectively.

The bottom graph plots the numerical outputs $(I_k, V(I_k, 5))$. The points on the second, third, fourth, and fifth graphs are nothing else but $(I_k, V(I_k, 5)ss(n)/ss(5))$, where $ss(n) = \sum_{j=1}^{n} S_j(n)^2/\lambda_j(n)$.

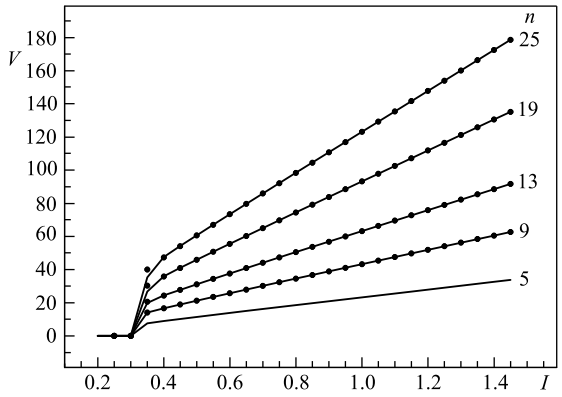

Fig. 3. The solid lines refer to back branches of the hysteresis loops, calculated numerically, for $n = 5, 9, 13, 19, 25$, from bottom to top, respectively. In all cases the right branch and the back branch of the hysteresis loops have been calculated numerically. The first graph plots the outputs $(I_k, V(I_k, 5))$. The circles on the other graphs are $(I_k, V(I_k, 5)ss(n)/ss(5))$, respectively. This confirms the possibility to obtain all the lines by simple similarity transforms of the bottom line

The occurrence of the factors $ss(n)/ss(5)$ can be motivated by the fact that, after the first iteration, we get $V(I, n) = ss(n)I/\beta$, and $1.45ss(n)$ is an excellent approximation to $V(1.45, n)$. We observe the same picture as at the end of [5], but the similarity transform coefficients here are $ss(n)/ss(5)$ instead of n.

CONCLUSIONS

The numerical results of IVC calculation and those obtained by the improved mixed numerical-analytical method are in good agreement with each other. The latter code is an order of magnitude faster and is free of computing error accumulation as well. The technicalities of the new method were described in Sec. 4 above.

Acknowledgements. The author is grateful to Yu. M. Shukrinov for the statement of the problem and useful discussions. Critical reading of the manuscript by Gh. Adam is acknowledged. The author is indebted to the referee for valuable critical comments which helped to clarify some details of the presentation.

REFERENCES

1. *Zappe H. H.* Minimum Current and Related Topics in Josephson Tunnel Junction Devices // J. Appl. Phys. 1973. V. 44, No. 3. P. 1371–1377.
2. *Matsuda Y. et al.* Collective Josephson Plasma Resonance in the Vortex State of $Bi_2Sr_2CaCu_2O_{8+\delta}$ // Phys. Rev. Lett. 1995. V. 75, No. 24. P. 4512–4515.
3. *Shukrinov Yu. M., Mahfousi F., Pedersen N. F.* Investigation of the Breakpoint Region in Stacks with a Finite Number of Intrinsic Josephson Junctions // Phys. Rev. B. 2007. V. 75. P. 104508.

4. *Serdyukova S. I.* Numerical-Analytical Method for Computing the Current-Voltage Characteristics for a Stack of Josephson Junctions // Comp. Math. Math. Phys. 2012. V. 52, No. 11. P. 1590–1596.
5. *Serdyukova S. I.* Determination of IVC Breakpoint for Josephson Junction Stack. Periodic and Non-Periodic with $\gamma = 0$ Boundary Conditions // Phys. Part. Nucl. Lett. 2013. V. 10, No. 3. P. 269–272.
6. *Bakhvalov N. S. et al.* Statics and Dynamics of Single-Electron Solitons in Two-Dimensional Arrays of Ultrasmall Tunnel Junctions // Physica B. 1991. V. 173, No. 3. P. 319–328.
7. *Bakhvalov N. S.* The Numerical Methods. M.: Nauka, 1973 (in Russian).
8. *Gantmacher F. R.* The Theory of Matrices. N. Y.: Chelsea Publ. Company, 1959.
9. *Hardy G. H., Rogosinski W. W.* Fourier Series. Cambridge Univ. Press, 1956.
10. *Levinson N.* Asymptotic Behavior of Solutions of Nonlinear Differential Equations // Studies in Appl. Math. 1969. V. XLVIII, No. 4.
11. REDUCE User's Guide for Unix Systems. Version 3.8 by Winfried Neun ZIB. 2004.

Received on July 18, 2013.